Journal Pre-proofs

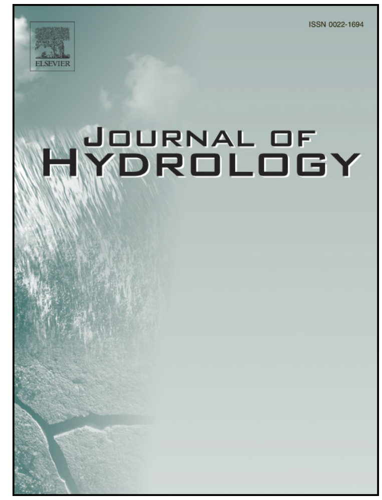

Research papers

Variations and Significance of Mg/Sr and $^{87}Sr/^{86}Sr$ in a Karst Cave System in Southwestern China

Jun-Yun Li, Ting-Yong Li, Chuan-Chou Shen, Tsai-Luen Yu, Tao-Tao Zhang, Yao Wu, Jing-Li Zhou, Chao-Jun Chen, Jian Zhang

PII: S0022-1694(21)00187-6
DOI: https://doi.org/10.1016/j.jhydrol.2021.126140
Reference: HYDROL 126140

To appear in: *Journal of Hydrology*

Received Date: 12 November 2020
Revised Date: 22 February 2021
Accepted Date: 23 February 2021

Please cite this article as: Li, J-Y., Li, T-Y., Shen, C-C., Yu, T-L., Zhang, T-T., Wu, Y., Zhou, J-L., Chen, C-J., Zhang, J., Variations and Significance of Mg/Sr and $^{87}Sr/^{86}Sr$ in a Karst Cave System in Southwestern China, *Journal of Hydrology* (2021), doi: https://doi.org/10.1016/j.jhydrol.2021.126140

Variations and Significance of Mg/Sr and $^{87}Sr/^{86}Sr$ in a Karst Cave System in Southwestern China

Jun-Yun Li [a, b] *，Ting-Yong Li [c] *，Chuan-Chou Shen [d]，Tsai-Luen Yu [d]，Tao-Tao Zhang [e, f]，Yao Wu [a], Jing-Li Zhou [a]，Chao-Jun Chen [a]，Jian Zhang [a, g]

[a] *Chongqing Key Laboratory of Karst Environment, School of Geographical Sciences, Southwest University, Chongqing 400715, China*

[b] *Key Laboratory of Karst Dynamics, MNR & Guangxi, Institute of Karst Geology, CAGS, Guilin, 541004，China*

[c] *Yunnan Key Laboratory of Plateau Geographical Processes & Environmental Changes, Faculty of Geography, Yunnan Normal University, Kunming 650500, China*

[d] *High-Precision Mass Spectrometry and Environment Change Laboratory (HISPEC), Department of Geosciences, National Taiwan University, Taipei 10617, Taiwan*

[e] *Key Laboratory of Alpine Ecology, Institute of Tibetan Plateau Research, Chinese Academy of Sciences, Beijing, 100101, China*

[f] *University of Chinese Academy of Sciences, Beijing100049, China*

[g] *Environnements et Paléoenvironnements Océaniques et Continentaux (EPOC), UMR CNRS, 5805, Université de Bordeaux, Pessac, France*

Revised to **Journal of Hydrology** **22, Feb., 2021**

*** Joint first and corresponding authors:**

Jun-Yun Li: jxljy@swu.edu.cn

Ting-Yong Li: cdlity@163.com

ABSTRACT

The geochemical compositions of cave drip water and speleothems such as Mg, Sr, Mg/Ca, Sr/Ca, and $^{87}Sr/^{86}Sr$ are considered to be responsive to changes in the local climate and hydrological conditions. Systematic monitoring was performed on the Mg and Sr contents, Mg/Sr ratio and $^{87}Sr/^{86}Sr$ of soil, soil water, cave drip water, and the active speleothems (AS) in Furong Cave in Chongqing, southwest China, during 2009–2018 (A.D). The results were interpreted in conjunction with the changes in the $^{87}Sr/^{86}Sr$ ratios to explore the main sources and controlling factors of Sr and other trace elements in drip water. (1) Due to the decrease in winter and spring rainfall, the residence time of water in the soil was prolonged, which resulted in increasing of Mg and Sr concentrations and $^{87}Sr/^{86}Sr$ ratios in soil water. It indicates that the trace element contents of soil water reflect seasonal changes of the rainfall. (2) The Mg and Sr contents were higher in drip water than in the soil water, as well as the $^{87}Sr/^{86}Sr$ of the cave drip-water was closer to that of the bedrock, which indicates that the overlying bedrock was the main source of the trace elements in the drip water and the speleothems in Furong Cave. (3) Mg contents and Mg/Sr ratios in drip water and AS showed decreasing trend, which may be affected by the shorter water-rock contact time due to the increasing annual rainfall in the monitoring period. (4) The Sr contents in AS might be affected by the growth rate of AS because of the similar increasing trend. (5) The Mg and Sr contents and the Mg/Sr ratios of the drip water and AS did not exhibit seasonal variations due to the mixing of the fissure water and complex hydrology condition of the overlying bedrock, however, the geochemical indexes (Mg and Mg/Sr ratio) showed an opposite trend to the annual rainfall variation. In short, this study highlights the responses of the changes of Mg, Sr and Mg/Sr ratios of drip water and AS to the rainfall on the multi-year timescale, which contributes critical insights into the paleoclimate interpretation of proxies of speleothems in the cave with hundreds of meters' thick bedrock.

KEYWORDS: Karst hydrology, Soil water, Drip water, Active speleothems, Mg/Sr, $^{87}Sr/^{86}Sr$

INTRODUCTION

When rainfall permeates through the soil, it dissolves CO_2 to form carbonic acid, which in turn dissolves the carbonate in the soil and bedrock. Drip water contains a variety of elements coming from the soil and bedrock. The information of environment is captured by the trace elements in drip water and speleothems in Karst caves (Fairchild et al., 2006, 2009). The Mg and Sr concentrations and the Mg/Ca and Sr/Ca ratios in drip water and speleothems are often used to explore climate and environmental changes (Hellstrom and McCulloch, 2000; McMillan et al., 2005; Li et al., 2005; Johnson et al., 2006; Cruz et al., 2007; Griffiths et al., 2010; Wong et al., 2011; Oster et al., 2012).

Studies tend to interpret possible annual to sub-annual climate signals in Mg/Ca, Sr/Ca and Ba/Ca of speleothems (Roberts et al., 1998; Fairchild et al., 2001; Treble et al., 2003; McDonald et al., 2004). It is possible that in caves covered by the bedrock tens/hundreds of meters thick (Bar-Matthews et al., 1996), or in caves with large entrances and the cave environment sensitive response to seasonal changes of temperature and humidity outside (Johnson et al., 2006), the element ratios (Mg/Ca and Sr/Ca) of drip water and speleothems can respond to seasonal variations of local temperature and rainfall. However, with regard to the caves covered by the bedrock tens of meters thick, a large amount of old water is stored in the complex bedrock fissures of the epikarst over the cave. The surface water is mixed in the process of infiltration, or due to the long flow path, the precipitation cannot form drip water in time. It has been assumed that water geochemistry variations due to seasonal changes in rainfall are unlikely to occur (Karmann et al., 2007). Nevertheless, in order to use element ratios in speleothems from relatively deep caves to reconstruct paleoclimate and paleoenvironment, it is concerned to know whether a climate signal exists in the trace elements of drip water, how trace element concentrations vary in soil water, drip water and active speleothem, as well as what the time scale of climate information change is recorded.

Cave monitoring is an important method to investigate the deposition mechanism and factor influencing the trace elements in drip water and speleothems (Fairchild et al., 2009). Previous studies have suggested that factors such as the external environment outside cave (air temperature and rainfall), the residence time of seepage water in the host rocks, PCP (prior calcite precipitation) along seepage water flow paths and the chemical composition of soil and bed rock changes the element ratios of drip water forming speleothems (Fairchild et al., 2000; Huang et al., 2001; Tooth and Fairchild, 2003; Musgrove and Banner, 2004; Fairchild et al., 2006; Wong et al., 2011; Huang et al., 2016; Zhang and Li, 2019). When performing a comprehensive study on a karst system, in addition to monitoring the internal cave environment, it is necessary to take into account the factors of local rainfall on recharge and on dissolution and precipitation processes occurring in karst systems (Smart and Friederich, 1987; Fairchild et al., 2000).

This article provides the cave monitoring data performing in Furong Cave which is covered by host rock with 300–500 m thick (Li et al., 2011) in southwestern China from 2009 to 2018 (A.D, after here, all the years mentioned in this article refer to the year of A.D). The variations of the contents of Mg and Sr and the ratios of Mg/Sr of soil, soil water, drip water and active speleothems have been systematically analyzed in the paper. The main sources of the trace elements in speleothems are explored according to the changes of $^{87}Sr/^{86}Sr$ values from soil to drip water, which is helpful to analyze the response mechanism of $^{87}Sr/^{86}Sr$ values of soil water and drip water to meteoric precipitation. We focus on discussing the relationship between the precipitation, soil, epikarst hydrology and the contents of Mg, Sr and Mg/Sr ratios variations in soil water, drip water and AS, and exploring the indexes response mechanisms to the changes of the surface environment at the multi-year time scale. Decades of monitoring data will help us to clarify the climate and environment significance of various proxy indexes in stalagmites from the deep caves and reconstructing paleoclimate quantitatively.

1. OVERVIEW OF THE STUDY AREA

Furong Cave (29°13′44″ N, 107°54′13″ E) is located in the Wulong District, Chongqing City, southwestern China (Figure 1A). The cave entrance is 480 m above sea level. The main hall is about 2,700 m long and is 30–50 m wide and high. Furong Cave was developed in Middle Cambrian limestone and dolomite formations. The region has a subtropical humid monsoon climate with the annual mean temperature and rainfall of 17.8°C and 1,064 mm (from 2009 to 2018), respectively. About 70–80% of the precipitation is concentrated between May and October (Li et al., 2011). In summer, the temperature is often high (maximum temperature >40°C) due to Subtropical High over the western Pacific. The surface soil overlying the cave is yellow subtropical mountain soil, which is 20–100 cm thick. The vegetation covering the cave are dominated by trees and shrubs (Li et al., 2012).

2. SAMPLE COLLECTION AND ANALYSIS

2.1 Sample collection

On both sides of the valley above the main hall of Furong Cave, five soil profiles (SA-SE) (Figure 1B) were chosen to collect soil samples from top to bottom at 5 cm intervals (except for intervals of 10 cm in the SC profile). A total of 8 bedrock samples were collected at the bottom of the SA-SE profiles. A water-collection tray made of PE was placed at the bottom of the soil profile to collect the soil water. The detailed methods of the soil water collection were described in Li et al. (2013). The soil water was collected in May-October, i.e., the period in which the regional rainfall is concentrated (Li et al., 2013).

Drip water in the main hall of Furong Cave was collected each month below six drip sites (MP1-MP5, MP9) as shown in Figure 1C (Li et al., 2011; Li and Li, 2018). PE (Polyethylene) bottles (50 mL) were immersed in 1:1 HCl for 24 h, washed with deionized water, and then dried before collecting soil water. The soil water samples were acidized with 0.1 mL of 7 M HNO_3 to maintain the ion activity (Li et al., 2013). A glass slide that had been cleaned as PE bottles was placed below each drip site to precipitate active speleothem (AS) samples and was replaced every three months. The AS samples were taken back to the laboratory and air-dried naturally, then weighed. By subtracting the weight of blank glass slide from the total weight, the mean AS deposition weight was obtained.

2.2 Methods

2.2.1 Samples analysis methods

We pre-processed the solid samples (e.g. soil, bedrock, and AS samples) by HF-$HClO_4$ heating digestion method. Samples were digested by using a mixture including 22.5 M HF, 12.38 M $HClO_4$, 6 M HCl, and 14 M HNO_3 to dissolve the solid particles completely. Then, the samples were diluted with 0.1 M HCl in PE bottles for the analysis of element concentration (Lu, 1999).

The treated solution and the soil water and drip water were analyzed to determine the contents of Ca, Mg and Sr using an Optima 2100DV inductively coupled plasma optical emission spectrometer (ICP-OES) (Perkin-Elmer, USA) with the detection limit of 1 μg/L and the relative error of less than 2% at the Geochemistry and Isotope Laboratory, School of Geographical Sciences, Southwest University.

Bedrock, soil samples were weighed into the Teflon beakers and dissolved completely using conventional HF-HNO3-HCl dissolution techniques in closed beakers. Soil water and drip water were filtered with a 0.45 μm filter and acidified with concentrated nitric acid. Sr was purified with Sr-Spec resin exchange columns, following the procedure described in Jung et al. (2019).The $^{87}Sr/^{86}Sr$ ratios were analyzed using a Multi-Collector Inductively-Coupled plasma Mass Spectrometer (MC-ICP-MS), Thermo Electron Finnigan Neptune, at the Department of Geosciences, National Taiwan University. The measured $^{87}Sr/^{86}Sr$ ratios were normalized to $^{86}Sr/^{88}Sr = 0.1194$ to correct for mass fractionation (Jung et al., 2019).

2.2.2 Data analysis method

Pearson correlation analysis was used to analyze the correlation of Mg and Sr in soil water, drip water and AS, respectively. The correlation coefficients between Mg and Sr are showed in the new Fig. 4.

Principal components analysis (PCA) was conducted to explore the driving factors of Mg and Sr changes in soil water (n=173), drip water (n=643) and AS (n=110). This method does not require normal distributions for large data sets (Kotowski, et al., 2020). The parameters are provided in Table 3.

3 RESULTS

According to Table 1, it was showed that the mean values (±1σ) of Mg and Sr contents and the Mg/Sr ratios were rainfall <soil water <drip water. But the maximum content of Mg and the Mg/Sr ratios are in rock, then in soil, and the minimum is in AS. Although the maximum content of Sr is in rock, but the minimum is in soil. The reasons were analyzed in section 4.1.

There were no seasonal variations of Mg and Sr contents in the soil water (Figure 2A and 2B) as well as the Mg/Sr ratios (Figure 2C). Nevertheless, the Mg and Sr contents of the soil water are significantly positively correlated (R=0.72, n=173, p<0.01) (Figure 4A), indicating that the dissolution of soil Mg and Sr may have been affected by the same factors.

From 2009 to 2018, the Mg, Sr contents and the Mg/Sr ratios of drip water exhibited similar trends at different drip sites, respectively (Figure 2D, 2E and 2F). The range of Mg was 6.66~47.65 mg/L (Table 1) and the monthly mean Mg contents showed an overall decrease trend (Figure 3A), as well as the monthly mean of Mg/Sr ratios (Figure 3C). During the whole monitoring period, the variation range of Sr concentration was between 0.021~0.077 mg/L (Table 1) and the trend line of the monthly mean Sr contents remained stable (Figure 3B). It is worth noting that the precipitation in the same period showed increasing trend (Figure 2G).

The Mg and Sr contents of the AS in Furong Cave underwent a two-stage change. (1) From 2009 to 2013, the Mg contents gradually decreased (mean content of 6,162 ± 1,081 μg/g), while the Sr contents continuously increased (mean content of 45.57 ± 15.98 μg/g). (2) From 2014 to 2016, both the Mg and Sr contents remained relatively stable (mean Mg content of 7,327 ± 1,314 μg/g and mean Sr content of 58.17 ± 12.29 μg/g) (Figure 5A, 5B). The Mg/Sr ratios decreased during 2009–2013 (mean ratio of 166.26 ± 61.98), while the ratios were relatively stable around a mean of 134.44 ± 36.68 during 2014–2016 (Figure 5C).

4 DISCUSSION

4.1 Main factors affecting the contents of Mg and Sr in soil water

The overlying bedrock of Furong Cave is mainly composed of limestone and dolomite, which are rich in Mg and poor in Sr (Table 1). The soil was developed from the bedrock. As water infiltrates into the soil, a large number of elements in the soil are dissolved and lost to the soil water, thereby resulting in the lower Mg and Sr contents of the soil compared with those of the bedrock (Table 1).

Mg is more chemically active than Sr, and soil clay particles exhibit strong Sr adsorption (Solecki and Michalik, 2006). Six types of limestone dissolution experiment showed that as the solution concentration of Mg and Sr increased, the dissolution rate of Mg was faster than that of Sr (Pracný et al., 2019). Therefore, after the surface rainwater infiltrates into the soil, the Mg and Sr contents of the soil water increase, but more Mg is dissolved than Sr over the same time interval, thereby leading to an increase in the Mg/Sr ratio of the soil water (Table 1).

The soil temperature and soil CO_2 concentration exhibit seasonal trends similar to that of the air temperature (Li et al., 2013; Li and Li, 2018). The mean Mg and Sr concentration of the soil water in March-April was 14.76 ± 8.35 mg/L and 0.023 ± 0.012 mg/L, respectively, while in May-October, the mean content of them was 12.80 ± 6.62 mg/L and 0.021 ± 0.009 mg/L, respectively. It has been known that the amount of soil water was in good agreement with the amount of rainfall (Li et al., 2013). During November to the following February, there was no soil water being collected (Figures 2A, 2B) attributing to the less rainfall (Li and Li, 2018, Figure 3F). In the seasons of low rainfall, infiltration water may stagnate for a long time in the soil porosities, which contributes to dissolving more CO_2 into the soil water and increasing the mineralization. When precipitation increases, more water infiltrates into soil and may lead to flushing trough the porosities. Therefore, the soil water collected in March-April had mixed the water which was held up in the winter with more Mg and Sr contents. From May to October, more rainfall results in less contact time between soil with infiltration water, which decreases the concentrations of Mg and Sr in the soil water. According the analysis results of Pearson correlation, there is a good positive correlation between Mg and Sr in soil water (Figure 4A). PCA analysis showed that two main factors controlled the content of Mg and Sr in soil water, one of which accounted for 86% (Table 3). Residence time may be the most important factor affecting the contents of Mg and Sr in soil water.

4.2 Analysis of control factors affecting Mg and Sr contents in drip water

The spring water above Furong Cave was characterized by $\delta^{13}C_{DIC}$ of -12‰ to -13‰ in summer and -5‰ to -6‰ in winter which are in phase with the wet and dry climate season (Li, et al., 2011). In other words, spring water can quickly respond to the change of precipitation. The mean contents of Ca, Mg and Sr in spring water were all higher than those in the soil water but lower than those in the drip water (Xiang et al., 2011). It is suggested that the infiltration water dissolves the elements from the limestone when it flows through the epikarst. But the contact time between spring water and the bedrock is short. Therefore, in the process of the infiltration water seeping into the fissures of the deeper bedrocks, more Mg and Sr are dissolved which results to increasing the Mg and Sr contents and the Mg/Sr ratios of the drip water (Table 1).

The air temperature in Furong Cave is 16.0~16.3°C throughout the year, which is similar to the local annual mean temperature (Li et al., 2011). Therefore, as the fissure water flows through the bedrock overlying Furong Cave, the effect of the temperature change on the element contents of the fissure water is negligible. Rainfall is another local environmental factor which is often taken into account in the process of fissure water dissolving the bedrock (Fairchild et al., 2000). However, there are no seasonal variations of Mg and Sr contents in drip water, as well as Mg/Sr ratios (Figure 2D, 2E and 2F). According the previous study in Furong Cave, many geochemical indicators of drip water (such as $\delta^{18}O$, $\delta^{13}C_{DIC}$, Mg/Ca and drip rate) lack seasonal variation due to the complicated hydrology conditions over the cave (Li et al., 2011; Li and Li, 2018; Zhang and Li, 2019), which have the function of regulating and storing fissure water. The fissure water are mixed in the bedrock resulting in the seasonal signal of precipitation being indistinct. Nevertheless, the drip rate responded to the annual rainfall (Zhang and Li, 2019). When the annual rainfall increased gradually, the drip rate increased as well, which shortened the residence time of the fissure water in the bedrock and in turn weakened the bedrock dissolution. It explained the decreasing trend of the mean Mg contents and Mg/Sr ratios of the drip water (Figure 3A, 3C) with the increasing rainfall during 2009 to 2018 (Figure 2G). Although there is a positive correlation between Mg and Sr of drip water (R=0.45) (Figure 4B), the decreasing trend of the mean Sr content was not obvious as that of Mg (Figure 3B). Only when the annual precipitation increased significantly, such as in 2015 and 2016, the content of Sr decreased as that of Mg (Figure 2D, 2E, 2F). In addition, PCA analysis also found that the most important factor affecting Mg and Sr accounted for 72.3% of two main factors in drip water, which was lower than in soil water (Table 3). It indicated that except the annual precipitation, the complicated hydrology condition in the epikarst overlying Furong Cave may have an important impact on Mg and Sr in drip water.

4.3 Variation characteristics and influencing factors of Mg and Sr in AS

The Mg contents and Mg/Sr ratios of the AS decreased from 2009 to 2013, while Sr contents increased. During 2014 to 2016, Mg, Sr and Mg/Sr ratios all remained relatively stable (Figure 5A, 5B and 5C). Though there is a positive correlation between Mg and Sr in AS, the correlation coefficient is lower than that of soil water and drip water (Figure 4). PCA analysis showed that the most important factor synchronously affecting Mg and Sr accounted for 68.9% of the whole influencing factors (Table 3). The contents of Mg and Sr in speleothem are mainly controlled by the precipitation process of calcite. In addition to the influence of Mg and Sr content in drip water, the environment in the cave such as humidity, temperature, pCO_2, dripping rate and the growth rate of speleothem all have influence on Mg and Sr entering into the calcium carbonate crystal (Paquette and Reeder, 1995; Goede et al., 1998; Fairchild et al., 2000; Hellstrom and McCulloch, 2000; Tooth and Fairchild, 2003; Treble et al.,2003; McDonald et al., 2004; Fairchild et al., 2006; Johnson et al., 2006). Even for a given factor, the influences on element Mg and Sr are different. For example, temperature has an effect on Mg, but has little effect on Sr (Gascoyne, 1983; Huang and Fairchild, 2001). Experiments have shown that the Sr partition coefficient K_{Sr} is strongly affected by the growth rate of calcium carbonate (Reeder and Grams, 1987; Paquette and Reeder, 1995; Stephenson et al., 2008). Gabitov et al. (2014) confirmed through experiments and GEM (growth entrapment model) simulations that K_{Sr} increased by a factor of six and K_{Mg} decreased by a factor of three as the calcium carbonate crystallization rate increased from 0.001 nm/s to 4 nm/s. Therefore, the correlation coefficient between Mg and Sr in AS was 0.38 which might be related to the comprehensive effect of multiple factors (Figure 4C).

The temperature and humidity in Furong Cave are stable all year around (Li, et al., 2011), however, the pCO$_2$ in the cave has seasonal variation (Li and Li, 2018). The average growth rate of six AS showed no seasonal characteristics but slowly increasing trend from 2009 to 2016 (Figure 5D), which is corresponded with the rainfall (Figure 5E). In section 4.2, it has been discussed that the decreasing trend of Mg in drip water is related to the shortened water-rock contact time with the increasing precipitation. The reduction of Mg in AS might be affected by the content of Mg in drip water. In addition, with the increase of growth rate, more Sr and less Mg may enter into the calcium carbonate crystals, which resulted in the decrease of Mg/Sr ratios in AS (Figure 5A, 5B, 5C).

4.4 Isotopic tracing with ^{87}Sr/^{86}Sr

The Sr contents and $^{87}Sr/^{86}Sr$ ratios of speleothems are commonly used in paleoclimate research (Banner et al., 1996; Goede et al., 1998; Bar-Matthews et al., 1999; Verheyden et al., 2000; Frumkin and Stein, 2004). The $^{87}Sr/^{86}Sr$ of stalagmites can be used to reveal the impacts of Sr sources on the $^{87}Sr/^{86}Sr$ of cave drip water (Faure and Mensing, 2005). Studies have shown that the overlying soil, bedrock, dust materials, and ocean spray are the main sources of Sr (Banner et al., 1996; Goede et al., 1998; Ayalon et al., 1999; Bar-Matthews et al., 1999; Verheyden et al., 2000; Frumkin and Stein, 2004; Li et al., 2005; Shand et al., 2009). Furong Cave is located in the mainland of China, about 850 km away from the nearest ocean (South China Sea). Therefore, the influence of ocean spray is negligible. Moreover, the Daba Mountains in the north and east of Sichuan Basin block the wind sand coming from the northwest, which results in the study region less affected by wind sand. Additionally, agricultural origin (fertilizers) may change (usually decrease) the isotope signature of Sr (Böhlke & Horan; 2000; Jiang et al., 2009; Jiang, 2011). According to our investigation, the upper of Furong Cave is in a relatively primitive state covered by dense vegetation and with little interference from human activities. Given that the Sr contents (mean of 0.008 mg/L) of local rainwater are much lower than those of the soil and soil water (Table

1), only the soil and bedrock were considered when investigating the factors influencing of the $^{87}Sr/^{86}Sr$ values of drip water.

The mean $^{87}Sr/^{86}Sr$ value of the overlying soil of Furong Cave was 0.72805 ± 0.00222, which is higher than the mean value of the underlying bedrock (0.70958 ± 0.00006) (Figure 6). The study area has a subtropical humid monsoon climate, with high temperatures and rainfall in summer and dense vegetation, and large amounts of CO_2 and other acidic substances are produced by soil respiration and microbial decomposition (Li et al., 2012; Li and Li., 2018). This results in strong chemical weathering of the soil and bedrock. Yang et al. (2001) proposed that the soil $^{87}Sr/^{86}Sr$ values reflect the intensity of the chemical weathering, with the ratios increasing with increasing weathering intensity. Therefore, the Sr supplied by soil that has undergone chemical weathering has higher $^{87}Sr/^{86}Sr$ values compared to that of the surrounding limestone (Li et al., 2005).

The $^{87}Sr/^{86}Sr$ values of all of the soil water and drip water fell between those of the soil and the bedrock (Figure 6). When rainwater infiltrates into the soil, it not only dissolves soil debris, but it also transports limestone debris with low $^{87}Sr/^{86}Sr$ ratios away (Banner et al., 1994; Borg and Banner, 1996), resulting in lower soil water $^{87}Sr/^{86}Sr$ values compared with those of the soil and bedrock.

The mean $^{87}Sr/^{86}Sr$ value of the cave drip water at drip sites MP1 and MP2 was closer to the mean bedrock $^{87}Sr/^{86}Sr$ value than the mean soil water $^{87}Sr/^{86}Sr$ value (Table 2, Figure 6). It is supposed that the evolution of $^{87}Sr/^{86}Sr$ ratios of groundwater from soil characteristics to that of bedrock reflects the occurrence of water rock interaction, which is related to the residence time of fissure water in bedrock (Musgrove and Banner, 2004; Oster et al., 2010; Wong et al., 2011; Wortham et al., 2017). The overlying bedrock of Furong Cave is 300–500 m thick which leads to longer water–rock interaction. In other words, the residence time of fissure water in the bedrock is the main factor affecting the trace element composition of the drip water.

4.5 Environmental implications of $^{87}Sr/^{86}Sr$

The mean $^{87}Sr/^{86}Sr$ value of the overlying soil of Furong Cave differs from that of the bedrock by 0.01847 (Table 2), while the $^{87}Sr/^{86}Sr$ of the soil water and drip water are between that of the soil and that of the bedrock (Figure 6), which reflected the change of the residence time of infiltration water in the soil and bedrock (Musgrove and Banner, 2004; Shand et al., 2007; Wong and Banner, 2010; Wong et al., 2011; Wortham et al., 2017). Comprehensive studies on the $^{87}Sr/^{86}Sr$ in modern stream waters, fast drip waters, and slow drip waters indicated that the faster the velocity, the lower Sr isotope ratio (Banner et al., 1996). According to the values in Table 2, the multi-month mean $^{87}Sr/^{86}Sr$ ratios of the soil water in soil profile SE in March–May and June–September were 0.71700 ± 0.00114 and 0.71242 ± 0.00072, respectively. The overlying soil water of Furong Cave mainly originates from rainfall, and thus, it quickly responds to the changes of rainfall (Li et al., 2013). From November to the following February, the soil water dries up due to the reduction in rainfall. Therefore, the soil water in March–May contains infiltrated water that has stayed in the soil for a long time and more detrital materials with high $^{87}Sr/^{86}Sr$ ratio were dissolved in soil water. The soil water in June–September mainly originates from the rainfall in the same month, resulting in the lower soil–water interaction time and a reduction of $^{87}Sr/^{86}Sr$ in soil water.

The cave drip water from sites MP1 and MP2 has similar $^{87}Sr/^{86}Sr$ values, which remained stable throughout the year without obvious seasonal variations (Table 2). Due to the limited number of $^{87}Sr/^{86}Sr$ measurements for the cave drip water and the short monitoring time (March-December, 2015), the regular $^{87}Sr/^{86}Sr$ pattern of the cave drip-water cannot be determined in detail.

Accordingly, the relationship between the $^{87}Sr/^{86}Sr$ of the cave drip water and the amount of rainfall is not addressed in this study.

5 CONCLUSIONS

During 2009-2018, the contents of Mg and Sr, Mg/Sr ratios and $^{87}Sr/^{86}Sr$ values from the soil and soil water overlying the cave, to the drip water and AS in Furong Cave, southwest China, were monitored. It is found that the trace element composition of the cave drip water mainly originates from the bedrock basing on the increase of the Mg and Sr contents from the soil water to the cave drip water, as well as the $^{87}Sr/^{86}Sr$ values of the cave drip-water closing to that of the bedrock. There were no seasonal variations of the Mg and Sr contents and Mg/Sr ratios in drip water and AS which are related to the complex karst system in the bedrock with hundreds of meters' thickness, however, Mg contents and Mg/Sr ratios responded to the change of regional rainfall on the multi-year timescale (Figure 2, 3 and 5).

Acknowledgements

This research was supported by the Open Project of Guangxi Key Science and Technology

Innovation Base on Karst Dynamics (KDL & Guangxi 202003) to J.-Y. Li, the National Natural Science Foundation of China (NSFC, No. 41772170; 42011530078), and the Fundamental Research Funds for the Central Universities, China (No. XDJK2017A010 and No. XDJK2020D005) to T.-Y. Li. This work also was supported by the Science Vanguard Research Program of the Ministry of Science and Technology (108-2119-M-002-012) and the Higher Education Sprout Project of the Ministry of Education, Taiwan (108L901001) to C. -C., Shen.

Author contributions:

J.-Y Li and T.-Y Li designed the research and wrote the manuscript. C. -C Shen and T.-L Yu complete the analyze of $^{87}Sr/^{86}Sr$. T.-T., Zhang, Y., Wu, J.-L., Zhou, C. -J Chen and J. Zhang did the field work and experiments. All authors discussed the results and provided ideas to input the manuscript.

Competing interests:

The authors declare no competing interests.

References

Ayalon, A., Bar-Matthews, M., Kaufman, A., 1999. Petrography, strontium, barium and uranium concentrations, and strontium and uranium isotope ratios in speleothems as palaeoclimatic proxies: Soreq Cave, Israel. Holocene 9, 715–722.

Banner, J.L., Musgrove, M. and Capo, R. C., 1994. Tracing groundwater evolution in a limestone aquifer using Sr isotopes: effects of multiple sources of dissolved ions and mineral-solution reactions. Geology 22, 687–690.

Banner, J.L., Musgrove, M., Asmerom, Y., Edwards, R.L., Hoff, J.A., 1996. High-resolution temporal record of Holocene ground-water chemistry: tracing links between climate and hydrology. Geology 24(11): 1049–1053.

Bar-Matthews, M., Ayalon A., Matthews, A., Sass, E. and Halicz, L., 1996. Carbon and oxygen isotope study of the active water carbonate system in a karstic Mediterranean cave: implications for paleoclimate research in semiarid regions. Geochimica et Cosmochimica. Acta 60, 337–347.

Bar-Matthews, M., Ayalon, A., Kaufman, A., Wasserburg, G.J., 1999. The Eastern Mediterranean paleoclimate as a reflection of regional events: Soreq cave, Israel. Earth and Planetary Science Letters 166, 85–95.

Böhlke, J.K., and Horan, M., 2000. Strontium isotope geochemistry of groundwaters and streams affected by agriculture, locust grove, MD. Applied Geochemistry 15: 599–609.

Borg, L. E., & Banner, J. L., 1996. Neodymium and strontium isotopic constraints on soil sources in Barbados, west Indies. Geochimica et Cosmochimica Acta, 60(21), 4193–4206.

Cruz Jr., F.W., Burns, S.J., Jercinovic, M., Karmann, I., Sharp, W.D., Vuille, M., 2007. Evidence of rainfall variations in Southern Brazil from trace element ratios (Mg/Ca and Sr/Ca) in a late Pleistocene stalagmite. Geochimica et Cosmochimica Acta 71, 2250–2263.

Fairchild, I.J., Baker, A., Borsato, A., Frisia, S., Hinton, R.W., McDermott, F., Tooth, A.F., 2001. High-resolution, multipletrace-element variation in speleothems. Journal of the Geological Society, London 158, 831–841.

Fairchild, I.J., Borsato, A., Tooth, A.F., Frisia, S., Hawkesworth, C.J., Huang, Y., McDermott, F., Spiro, B., 2000. Controls on trace element (Sr–Mg) compositions of carbonate cave waters: implications for speleothem climatic records. Chemical Geology 166, 255–269.

Fairchild, I.J., Smith, C.L., Baker, A., Fuller, L., Spötl, C., Mattey, D., McDermott, F., E.I.M.F., 2006. Modification and preservation of environmental signals in speleothems. Earth-Science Reviews, 75: 105–153.

Fairchild, I.J., Treble, P., 2009. Trace elements in speleothems as recorders of environmental change. Quaternary Science Reviews 28, 449–468.

Faure, G., Mensing, T.M., 2005. Isotopes: Principles and Applications. Wiley, Hoboken.

Frumkin, A., Stein, M., 2004. The Sahara-East Mediterranean dust and climate connection revealed by strontium and uranium isotopes in a Jerusalem speleothem. Earth and Planetary Science Letters 217, 451–464.

Gabitov, R.I., Sadekov, A., Leinweber, A., 2014. Crystal growth rate effect on Mg/Ca and Sr/Ca partitioning between calcite and fluid: An in situ approach. Chemical Geology 367:70–82.

Gascoyne, M., 1983. Trace element partition coefficients in the calcite-water system and their paleoclimatie significance in cave studies. Journal of Hydrology 61, 213-222.

Goede, A., McCulloch, M., McDermott, F., Hawkesworth, C., 1998. Aeolian contribution to strontium and strontium isotope variations in a Tasmanian speleothem. Chemical Geology 149, 37–50.

Griffiths, M.L., Drysdale, R.N., Gagan, M.K., Frisia, S., Zhao, J.X., Ayliffe, L.K., Hantoro, W.S., Hellstrom, J.C., Fischer, M.J., Feng, Y.X., Suwargadi, B.W., 2010. Evidence for Holocene changes in Australian–Indonesian monsoon rainfall from stalagmite trace element and stable isotope ratios. Earth and Planetary Science Letters 292 (1–2), 27–38.

Hellstrom, J., McCulloch, M.T., 2000. Multi-proxy constraints on the climatic significance of trace element records from a New Zealand speleothem. Earth and Planetary Science Letters 179, 287–297.

Huang, W., Wang, Y.J., Cheng, H., Edwards, R.L., Shen, C.C., Liu, D., Shao, Q., Deng, C., Zhang, Z., Wang, Q., 2016. Multi-scale Holocene Asian Monsoon variability deduced from a twin-stalagmite record in southwestern China. Quat. Res. 86 (1), 34–44.

Huang, Y., Fairchild, I.J., 2001. Partitioning of Sr^{2+} and Mg^{2+} into calcite under arstanalogue experimental conditions. Geochimica et Cosmochimica Acta 65, 47–62.

Jiang, Y.J., 2011. Strontium isotope geochemistry of groundwater affected by human activities in Nandong underground river system, china. Applied Geochemistry 26(3), 371–379.

Jiang, Y.J., W, Y.X., Yuan, D.X., 2009. Human impacts on karst groundwater contamination deduced by coupled nitrogen with strontium isotopes in the nandong underground river system in yunan, china. Environmental Science & Technology 43 (20): 7676–7683.

Johnson, K.R., Hu, C., Belshaw, N.S., Henderson, G.M., 2006. Seasonal trace-element and stable-isotope variations in a Chinese speleothem: the potential for high resolution paleomonsoon reconstruction. Earth and Planetary Science Letters 244(1–2), 394–407.

Jung, C.C., Chou, C.K., Lin, C.Y., Shen, C.C., Lin, Y.C., Huang, Y.T., Tsai, C.Y., Yao, P.H., Huang, C.R., Huang, W.R., Chen, M.J., Huang, S.H., Chang, S.C., 2019. C-Sr-Pb isotopic characteristics of $PM_{2.5}$ transported on the East-Asian continental outflows. Atmospheric Research 223, 88-97.

Karmann, I., Cruz, F.W., Viana, O., Burns, S.J., 2007. Climate influence on geochemistry parameters of waters from Santana–Pérolas cave system, Brazil. Chemical Geology, 244(1-2), 232–247.

Kotowski, T., Motyka, J., Knap, W., Bielewski, J., 2020. 17-year study on the chemical composition of rain, snow and sleet in very dusty air (Krakow, Poland). Journal of Hydrology 582, 124543.

Li, H., Ku, T., You, C., Cheng, H., Edwards, R., Ma, Z., Tsai, W., Li, M., 2005. $^{87}Sr/^{86}Sr$ and Sr/Ca in speleothems for paleoclimate reconstruction in Central China between 70 and 280 kyr ago. Geochimica & Cosmochimica Acta 69, 3933–3947.

Li, J.-Y., Li, T.-Y., 2018. Seasonal and annual changes in soil/cave air pCO_2 and the $\delta^{13}C_{DIC}$ of cave drip water in response to changes in temperature and rainfall. Applied Geochemistry 93, 94–101.

Li, J.Y., Li, T.Y., Wang, J.-L., Xiang, X.X., Chen, Y.X., Li, X., 2013. Characteristics and environmental significance of Ca, Mg and Sr in the soil infiltrating water overlying the Furong Cave, Chongqing, China. Science China: Earth Sciences 56(12), 2126–2134.

Li, T.Y., Li, H.C., Xiang, X.J., Kuo, T.S., Li, J.Y., Zhou, F.L., Chen, H.L., Peng, L.L., 2012. Transportation characteristics of $\delta^{13}C$ in the plants-soil-bedrock-cave system in Chongqing karst area. Science China Earth Sciences 55: 685–694.

Li, T.-Y., Shen, C.-C., Li, H.-C., Li, J.-Y., Chiang, H.-W., Song, S.-R., Yuan, D.-Y., Chris, D.J. Gao, L.-P., Zhou, L.-P., Wang, J.-L., Ye, M.-Y., Tang, L.-L., Xie, S.-Y., 2011. Oxygen and carbon isotopic systematics of aragonite speleothems and water in Furong Cave, Chongqing, China. Geochimica & Cosmochimica Acta 75: 4140–4156.

Lu, R.K., 1999. Analysis Methods of Soil Agricultural Chemistry (in Chinese). Beijing: China

Agricultural Science and Technology Publishing House.147–211.

McDermott, F., 2004. Palaeo-climate reconstruction from stable isotope variations in speleothems: a review. Quaternary Science Reviews 23, 901–918.

McMillan, E.A., Fairchild, I.J., Frisia, S., Borsato, A., McDermott, F., 2005. Annual trace element cycles in calcite–aragonite speleothems: evidence of drought in the western Mediterranean 1200–1100 yr BP. Journal of Quaternary Science 20 (5), 423–433.

Musgrove, M., Banner, J.L., 2004. Controls on the spatial and temporal variability of vadose dripwater geochemistry: Edwards Aquifer, central Texas. Geochimica & Cosmochimica Acta 68 (5), 1007–1020.

Oster, J.L., Montañez, I.P., Guilderson, T.P., Sharp, W.D., Banner, J.L., 2010. Model-ing speleothem δ13C variability in a central Sierra Nevada cave using 14C and 87Sr/86Sr. Geochimica & Cosmochimica Acta 74: 5228–5242.

Oster, J.L., Montañez, I.P., Kelley, N.P., 2012. Response of a modern cave system to large seasonal precipitation variability. Geochimica & Cosmochimica Acta 91, 92–108.

Paquette, J., Reeder, R.J., 1995. Relationship between surface structure, growth mechanism, and trace element incorporation in calcite. Geochimica & Cosmochimica Acta 59, 735–749.

Pracný, P., Faimon, J., Všianský, D., Přichystal, A., 2019. Evolution of Mg/Ca Ratios During the experimental dissolution of limestone. Chemical Geology 523:107–120.

Reeder, R.J., Grams, J.C., 1987. Sector zoning in calcite cement crystals: implications for trace element distributions in carbonates. Geochimica & Cosmochimica Acta 51, 187–194.

Shand, P., Darbyshire, D.P.F., Gooddy, D.C., Haria, A.H., 2007. $^{87}Sr/^{86}Sr$ as an indicator of flow paths and weathering rates in the Plynlimon experimental catchments, Wales. UK. Chem. Geol. 236, 247–265.

Shand, P., Darbyshire, D.P.F., Love, A.J., Edmunds, W.M., 2009. Sr isotopes in natural waters: applications to source characterisation and water–rock interaction in contrasting landscapes. Applied Geochemistry, 24(4), 574–586.

Smart, P. L and Friederich, H. 1987. Water movement and storage in the unsaturated zone of a maturely karstified aquifer, Mendip Hills, England. In Proceedings of the Conference on Environmental Problems in Karst Terrains and their Solutions. 59-87.

Solecki, J., Michalik, S., 2006. Studies of ^{85}Sr adsorption on grain fractions of soil. Journal of Radio analytical and Nuclear Chemistry 267(2): 271–278.

Stephenson, A.E., DeYoreo, J.J., Wu, L., Wu, K.J., Hoyer, J., Dove, P.M., 2008. Peptides enhance magnesium signature in calcite: insights into origins of vital effects. Science 322, 724–727.

Tooth, A.F., Fairchild, I.J., 2003. Soil and karst aquifer hydrological controls on the geochemical evolution of speleothem-forming drip waters, Crag Cave, southwest Ireland. Journal of Hydrology 273, 51–68.

Treble, P., Shelley, J.M.G., Chappell, J., 2003. Comparison of high resolution sub-annual records of trace elements in a modern (1911–1992) speleothem with instrumental climate data from southwest Australia. Earth and Planetary Science Letters 216, 141–153.

Verheyden, S., Keppens, E., Fairchild, I.J., McDermott, F., Weis, D., 2000. Mg, Sr and Sr isotope geochemistry of a Belgian Holocene speleothem: implications for paleoclimate reconstructions. Chemical Geology 169, 131–144.

Wong, C. I., Banner, J. L., Musgrove, M., 2011. Seasonal dripwater Mg/Ca and Sr/Ca variations driven by cave ventilation: Implications for and modeling of speleothem paleoclimate records. Geochimica & Cosmochimica Acta 75, 3514–3529.

Wong, C., Banner, J.L., 2010. Response of cave air CO_2 and drip water to brush clearing in central

Texas: implications for recharge and soil CO_2 dynamics. Journal of Geophysical Research 115, G04018. doi: 10.1029/2010JG001301.

Wortham, B.E., Wong, C.I., Silva, L.C.R., McGee, D., Montañez, I.P., Troy Rasbury, E., Rasbury, E.T., Cooper, K.M., Sharp, W.D., Glessner, J.G., Santos, R.V., 2017. Assessing response of local moisture conditions in central brazil to variability in regional monsoon intensity using speleothem $^{87}Sr/^{86}Sr$ values. Earth & Planetary Science Letters, 463(Complete), 310–322.

Xiang, X.J., Li, T.Y., Wang, J.L., Li, J.Y., Chen, Y.X., Zhou, F.L., Huang, X., 2011. Variation characteristics of elements in soil infiltrating water-drips around Furong Cave of Chongqing and their implications. Journal of Soil and Water Conservation 25 (3), 121-125.

Yang, J.D., Chen, J., Tao, X.C., Li, C.L., Ji, J.F., Chen, Y., 2001. Sr isotope ratios of acid leached loess residues from Luochuan, China: A tracer of continental weathering intensity over the past 2.5 Ma. Geochemical Journal 35(6): 403– 412 .

Zhang, J., and Li, T. -Y., 2019. Seasonal and interannual variations of hydrochemical characteristics and stable isotopic compositions of drip waters in Furong Cave, Southwest China based on 12 years' monitoring. Journal of Hydrology 572: 40–50.

Captions

Figure 1 (A) Location of the study area, Furong Cave in Southwest China. The circle indicates the location of Chongqing City. The black solid dot indicates the location of Furong Cave. Yangtze River flows across Chongqing municipality city from the southwest to the northeast (modified after Li et al., 2011). (B) Distribution of soil profiles and the monitoring sites of soil water over Furong Cave (SA-SE, the black triangles). The black shadow indicates the Furong Cave; contours with elevations for this area are shown (modified after Li et al., 2013). (C) Sketch map of the Furong Cave. Distribution of the monitoring sites: MP1-MP5 and MP9 for drip water (black solid stars). The sites of MP1-MP3 and MP9 are all located in the Great Hall. MP4 and MP5 are in the corridor, approximately 600 m from the entrance. The dashed line shows the tour route and the Great Hall indicates the inner part of the cave (modified after Li et al., 2011, 2018).

Figure 2 In-phase variations of trace elements and Mg/Sr time series in soil water and drip water at Furong Cave. (A-C) Comparisons of the concentration of Mg (A), Sr (B) and the ratios of Mg/Sr (C) of soil water (no data in 2013) above Furong Cave in the period of 2009-2016 (A.D.). (D-F) the concentration of Mg (D), Sr (E) and the ratios of Mg/Sr (F) of drip water during 2009-2018 (A.D.). (G) monthly average temperature (red curve) and annual precipitation (blue columns) outside of Furong Cave. The gray dashed lines with arrows denote the long-term trends for changes of precipitation. There was no obvious seasonal change in the contents of Mg and Sr and Mg/Sr ratios in soil water.

Figure 3 The variation trend of the monthly average contents of Mg (A) and Sr (B) and Mg/Sr ratios (C) in drip water during 2009 to 2018. The red dotted line in the figure is automatically generated by statistical analysis, indicating the variation trend of the average values. It is showed that the decreasing trend of the monthly average Mg contents and Mg/Sr ratios of the drip water (Figure 3A, 3C) with the increasing rainfall during 2009 to 2018 (Figure 2G), but the contents of Sr have no obvious change (Figure 3B).

Figure 4 The significant positive correlation between the concentration of Mg and Sr in soil water (A) above Furong Cave, drip water (B) and AS (C) in the cave.

Figure 5 Time series of the concentration of Mg (A), Sr (B), the ratios of Mg/Sr (C) and the average growth rate of active speleothem with standard error of the mean (uncertainty bars) (D). The interrupted dashed red line in panel (D) indicates the trend of average growth rate of active speleothem, which was consistent with the trend of annual precipitation outside of Furong Cave (E). The gray dashed lines with arrows in (A, B, C, E) denote the trends for changes in the monitoring parameters.

Figure 6 $^{87}Sr/^{86}Sr$ values of bedrock (n=2), soils (n = 12), and soil water (n = 6) above Furong Cave, and drip water (n = 19) in Furong Cave. Uncertainty bars are standard error of the mean values. Complete data are listed in Table 2.

Abstract

The geochemical compositions of cave drip water and speleothems such as Mg, Sr, Mg/Ca, Sr/Ca, and $^{87}Sr/^{86}Sr$ are considered to be responsive to changes in the local climate and hydrological conditions. Systematic monitoring was performed on the Mg and Sr contents, Mg/Sr ratio and $^{87}Sr/^{86}Sr$ of soil, soil water, cave drip water, and the active speleothems (AS) in Furong Cave in Chongqing, southwest China, during 2009–2018 (A.D). The results were interpreted in conjunction with the changes in the $^{87}Sr/^{86}Sr$ ratios to explore the main sources and controlling factors of Sr and other trace elements in drip water. (1) Due to the decrease in winter and spring

rainfall, the residence time of water in the soil was prolonged, which resulted in increasing of Mg and Sr concentrations and $^{87}Sr/^{86}Sr$ ratios in soil water. It indicates that the trace element contents of soil water reflect seasonal changes of the rainfall. (2) The Mg and Sr contents were higher in drip water than in the soil water, as well as the $^{87}Sr/^{86}Sr$ of the cave drip-water was closer to that of the bedrock, which indicates that the overlying bedrock was the main source of the trace elements in the drip water and the speleothems in Furong Cave. (3) Mg contents and Mg/Sr ratios in drip water and AS showed decreasing trend, which may be affected by the shorter water-rock contact time due to the increasing annual rainfall in the monitoring period. (4) The Sr contents in AS might be affected by the growth rate of AS because of the similar increasing trend. (5) The Mg and Sr contents and the Mg/Sr ratios of the drip water and AS did not exhibit seasonal variations due to the mixing of the fissure water and complex hydrology condition of the overlying bedrock, however, the geochemical indexes (Mg and Mg/Sr ratio) showed an opposite trend to the annual rainfall variation. In short, this study highlights the responses of the changes of Mg, Sr and Mg/Sr ratios of drip water and AS to the rainfall on the multi-year timescale, which contributes critical insights into the paleoclimate interpretation of proxies of speleothems in the cave with hundreds of meters' thick bedrock.

Author contributions：

J.-Y Li and T.-Y Li designed the research and wrote the manuscript. C. -C Shen and T.-L Yu complete the analyze of $^{87}Sr/^{86}Sr$. T.-T., Zhang, Y., Wu, J.-L., Zhou, C. -J Chen and J. Zhang did the field work and experiments. All authors discussed the results and provided ideas to input the manuscript.

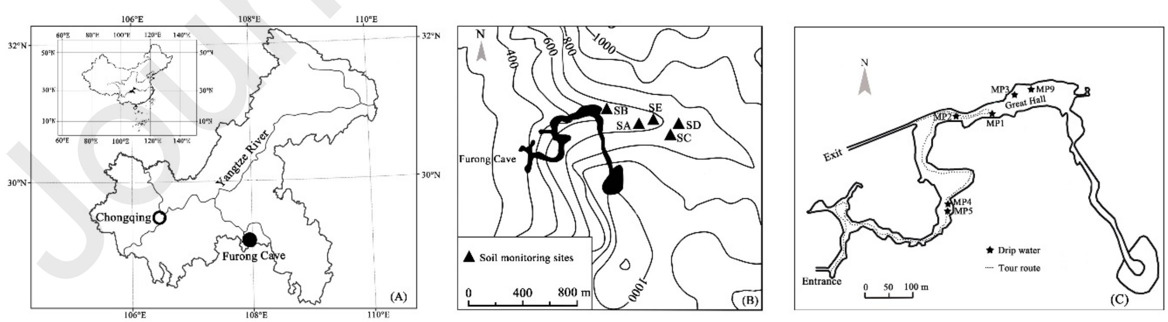

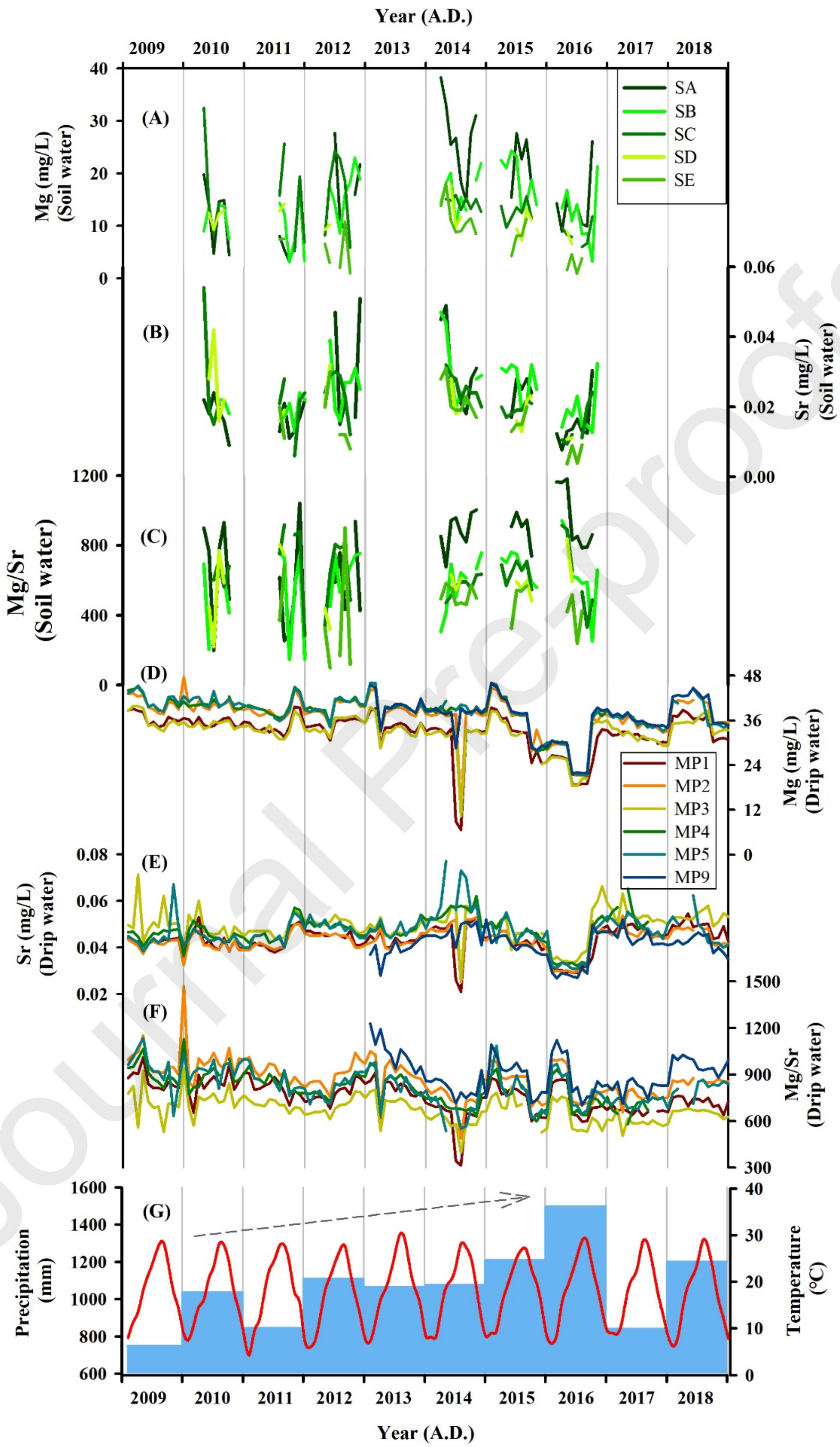

Year (A.D.)
2009
2010
2011
2012
2013
2014
2015
2016
2017
2018
Mg (mg/L)
(Soil water)
(A)
SA
SB
SC
SD
SE
(B)
Sr (mg/L)
(Soil water)
(C)
Mg/Sr
(Soil water)
(D)
Mg (mg/L)
(Drip water)
MP1
MP2
MP3
MP4
MP5
MP9
(E)
Sr (mg/L)
(Drip water)
(F)
Mg/Sr
(Drip water)
(G)
Precipitation
(mm)
Temperature
(°C)

582

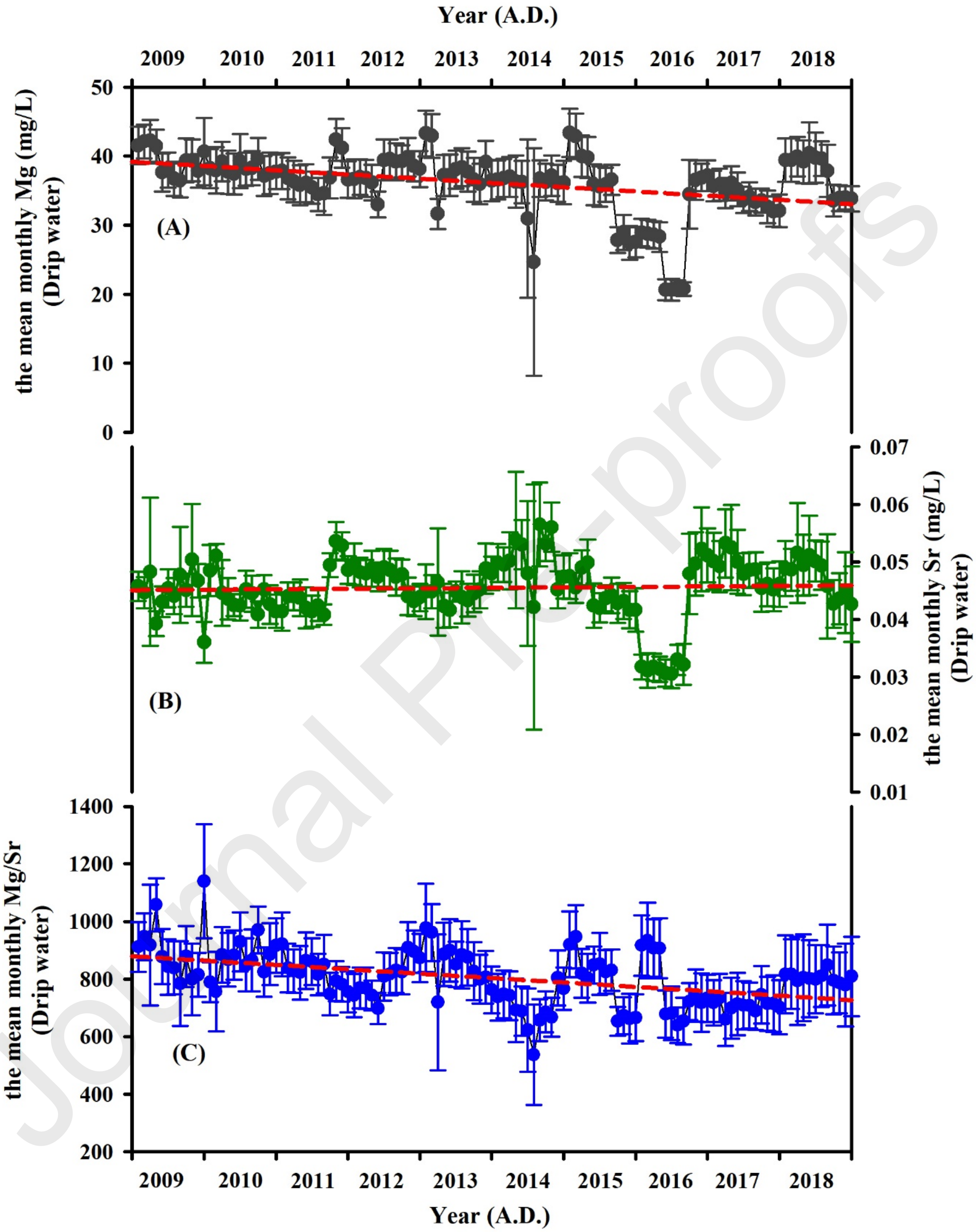
Year (A.D.)
2009 2010 2011 2012 2013 2014 2015 2016 2017 2018
the mean monthly Mg (mg/L) (Drip water)
0 10 20 30 40 50
(A)
(B)
the mean monthly Sr (mg/L) (Drip water)
0.01 0.02 0.03 0.04 0.05 0.06 0.07
the mean monthly Mg/Sr (Drip water)
200 400 600 800 1000 1200 1400
(C)
2009 2010 2011 2012 2013 2014 2015 2016 2017 2018
Year (A.D.)

583

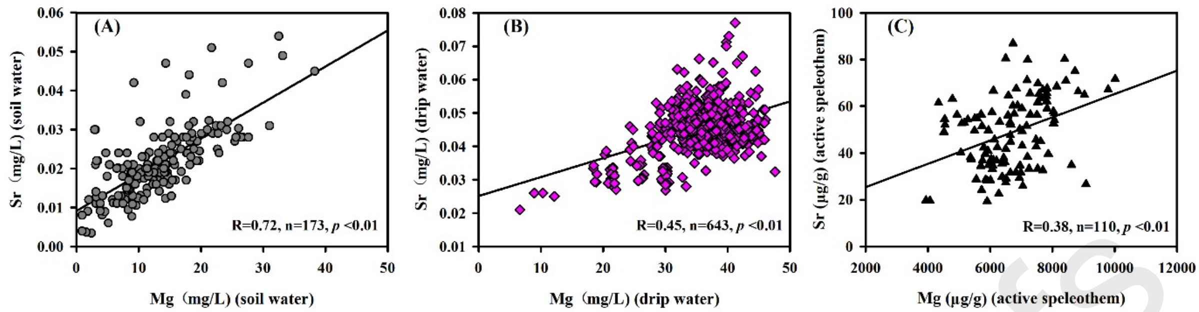
(A)
Sr（mg/L) (soil water)
Mg（mg/L) (soil water)
R=0.72, n=173, p <0.01
(B)
Sr（mg/L) (drip water)
Mg（mg/L) (drip water)
R=0.45, n=643, p <0.01
(C)
Sr (μg/g) (active speleothem)
Mg (μg/g) (active speleothem)
R=0.38, n=110, p <0.01

584

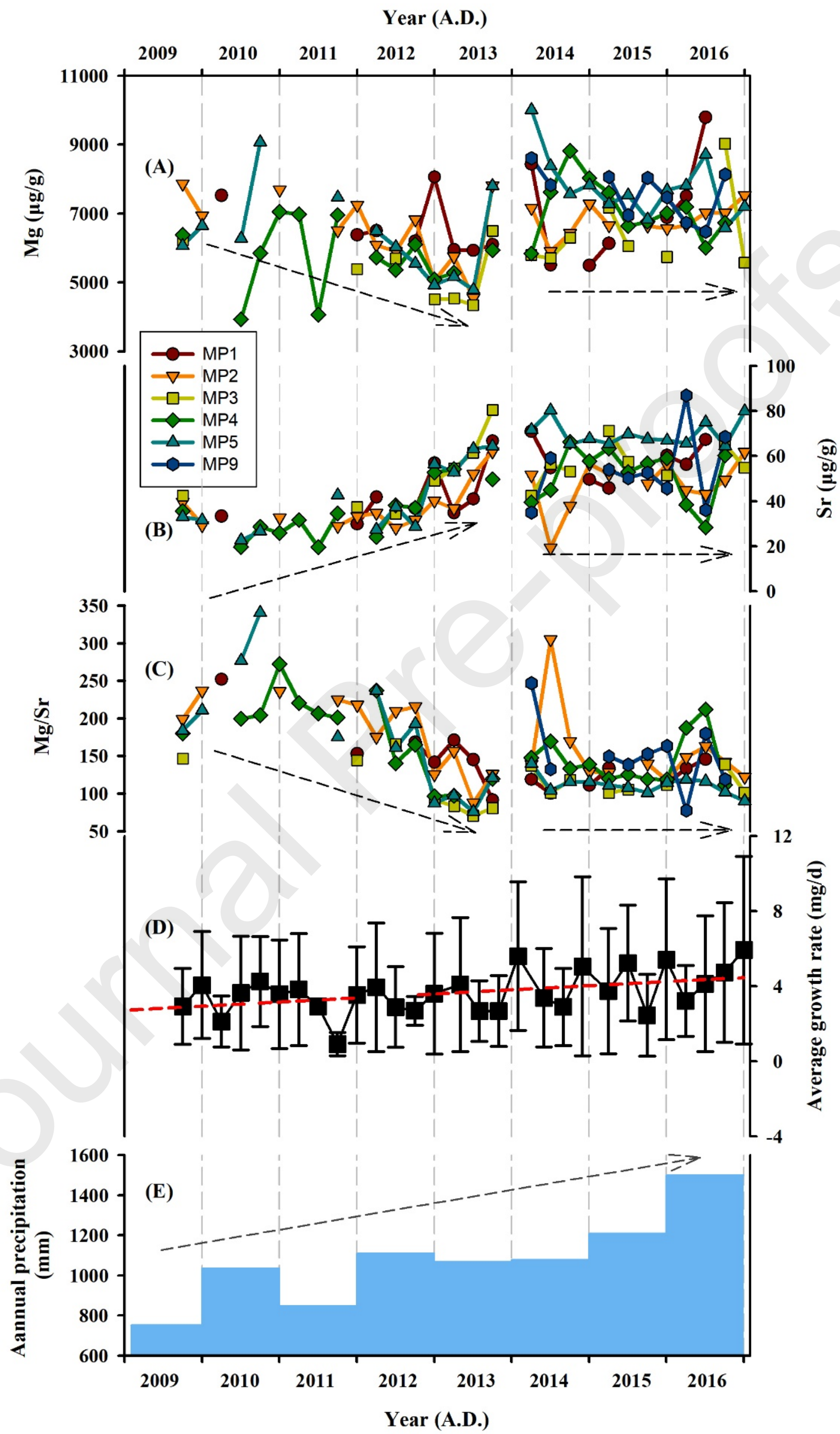
Year (A.D.)
2009
2010
2011
2012
2013
2014
2015
2016
Mg (µg/g)
(A)
MP1
MP2
MP3
MP4
MP5
MP9
Sr (µg/g)
(B)
Mg/Sr
(C)
(D)
Average growth rate (mg/d)
Aannual precipitation (mm)
(E)

585

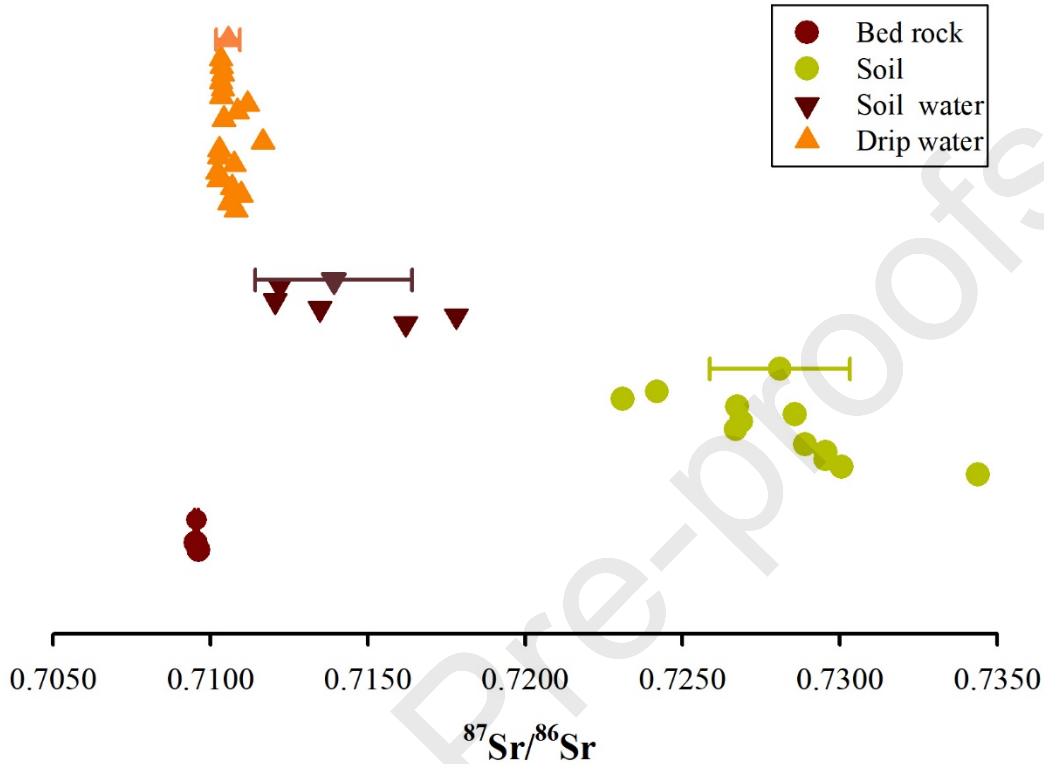

Table 1 Mean concentration of Mg, Sr and Mg/Sr ratios in bedrocks, soil, soil water, drip water and active speleothem from Furong Cave.

mple （unit）	n	Mg			Sr			Mg/Sr	
		max	mean	min	max	mean	min	max	mean
mg/L)	6	0.285	0.214±0.069	0.123	0.015	0.008±0.004	0.003	46	29±9
µg/g)	56	96459	18929±16921	5999	79.00	47.74±9.4	25.80	1221	371±233
ater (mg/L)	174	38.31	13.22±6.78	0.92	0.067	0.022±0.009	0.003	1181	617±223
(µg/g)	8	145158	131117±8927	119172	186	125±38	75	1940	1152±411
ater (mg/L)	643	47.65	35.94±5.56	6.66	0.077	0.045±0.007	0.021	1470	800 ± 133
e speleothems (µg/g)	114	11793	6770±1336	3931	87.87	49.88±16.42	19.34	341	150±53

590 **Table 2 $^{87}Sr/^{86}Sr$ ratios in bedrocks, soil, soil water and drip water**

Month of Sampling in 2015 (A.D)	Sample ID	Sample Type	Detail information	$^{87}Sr/^{86}Sr$	Mean of $^{87}Sr/^{86}Sr$
May	SE-R	Bedrock	profile SE	0.70962	0.70958± 0.00006
	SD-R		profile SD	0.70954	
May	SE01	Soil	0-3 cm	0.73438	0.72805±0.00222
	SE03		6-9 cm	0.73005	
	SE08		20-22 cm	0.72953	
	SE13		30-32 cm	0.72954	
	SE17		38-40 cm	0.72889	
			Mean value	**0.73048±0.00222**	
May	SD01	Soil	0-5 cm	0.72668	
	SD03		10-15 cm	0.72685	
	SD07		30-35 cm	0.72857	
	SD11		50-55 cm	0.72673	
	SD15		66-69 cm	0.72310	
	SD20		81-84 cm	0.72418	
			Mean value	**0.72602±0.00200**	
March	SE-201503	Soil water	profile SE	0.71619	0.71394± 0.00249
May	SE-201505			0.71781	
June	SE-201506			0.71349	
July	SE-201507			0.71206	
August	SE-201508			0.71192	
September	SE-201509			0.71219	
March	MP1-201503	Drip water	MP1	0.71081	0.71059 ± 0.00038
April	MP1-201504			0.71060	
May	MP1-201505			0.71098	
June	MP1-201506			0.71068	
July	MP1-201507			0.71027	
August	MP1-201508			0.71023	
September	MP1-201509			0.71076	
October	MP1-201510			0.71028	
November	MP1-201511			0.71028	
December	MP1-201512			0.71167	
			Mean value	**0.71066 ± 0.00045**	
April	MP2-201504	Drip water	MP2	0.71042	
May	MP2-201505			0.71086	
June	MP2-201506			0.71118	
July	MP2-201507			0.71034	
August	MP2-201508			0.71040	
September	MP2-201509			0.71034	

October	MP2-201510		0.71040
November	MP2-201511		0.71035
December	MP2-201512		0.71034
		Mean value	**0.71052 ± 0.00030**

Table 3 PCA analysis results on Mg and Sr data of soil water, drip water and AS (active speleothem)

	Soil water (n=173)		**Drip water** (n=643)		**AS** (n=110)	
	*Comp.1	Comp.2	Comp.1	Comp.2	Comp.1	Comp.2
Standard deviation	1.311	0.528	1.202	0.743	1.174	0.788
Proportion of Variance	0.860	0.140	0.723	0.277	0.689	0.311
Cumulative Proportion	0.860	1.00	0.723	1.00	0.689	1.00

*Comp.1, Comp.2, represent the calculated principal components, Standard deviation represents the Standard deviation of each principal component, Proportion of Variance represents the contribution rate of each principal component, Cumulative Proportion represents the Cumulative contribution rate of each principal component.

Highlights

1 Ten years monitoring work in a karst cave overlying 300-500 meters' bedrock.

2 Bedrock is the main source of the trace elements in the drip water and speleothems.

3 Increase rainfall results in decreased Mg, Mg/Sr ratio, and increase in Sr content.